Observation of isomeric states in neutron deficient $A\sim80$ nuclei following the projectile fragmentation of ^{92}Mo

C. Chandler,[1] P. H. Regan,[1] B. Blank,[2] C. J. Pearson,[1] A. M. Bruce,[3] W. N. Catford,[1] N. Curtis,[1,*] S. Czajkowski,[2] Ph. Dessagne,[4] A. Fleury,[2] W. Gelletly,[1] J. Giovinazzo,[2,4] R. Grzywacz,[5,6] Z. Janas,[2,5] M. Lewitowicz,[6] C. Marchand,[2] Ch. Miehé,[4] N. A. Orr,[7] R. D. Page,[8] M. S. Pravikoff,[2] A. T. Reed,[8] M. G. Saint-Laurent,[6] S. M. Vincent,[1,†] R. Wadsworth,[9] D. D. Warner,[10] J. S. Winfield,[1,6] and F. Xu[1]

[1]*School of Physical Sciences, University of Surrey, Guildford, GU2 5XH, United Kingdom*
[2]*CEN Bordeaux-Gradignan, Le Haut-Vigneau, F-33175 Gradignan Cedex, France*
[3]*School of Engineering, University of Brighton, Brighton, BN2 4GJ, United Kingdom*
[4]*IReS, BP28, F-67037 Strasbourg Cedex, France*
[5]*Institute of Experimental Physics, Warsaw University, Pl-00681 Warsaw, Poland*
[6]*GANIL, BP 5027, F-14000 Caen Cedex, France*
[7]*LPC, ISMRA et Université de Caen, Bld. du Marechal Juin, 14050 Caen Cedex, France*
[8]*Department of Physics, Oliver Lodge Laboratory, University of Liverpool, Liverpool, L69 7ZE, United Kingdom*
[9]*Department of Physics, University of York, Heslington, York, Y01 4DD, United Kingdom*
[10]*CLRC Daresbury Laboratory, Warrington, WA4 4AD, United Kingdom*

(Received 13 August 1999; published 3 March 2000)

γ-ray decays depopulating isomeric states have been observed in a number of very neutron deficient nuclei around $A\sim80$ following the projectile fragmentation of a ^{92}Mo primary beam. Previously unobserved decays have been identified in the $N=Z+2$ nuclei $^{80}_{39}$Y and $^{84}_{41}$Nb and the $N=Z$ nucleus, $^{86}_{43}$Tc, making the latter the heaviest $N=Z$ nucleus to date in which a discrete γ-ray transition has been assigned. The lifetime of the previously reported $I^{\pi}=\frac{9}{2}^{+}$ isomeric state in ^{73}Kr has also been measured and a clearer picture of its decay properties has been deduced. Isomeric ratios have been measured and have been interpreted in terms of the yrast or nonyrast nature of the isomeric state.

PACS number(s): 21.10.Tg, 25.70.Mn, 27.50.+e

I. INTRODUCTION

The richness observed in the structure of the neutron deficient nuclei with $A\sim80$ is the result of the low level density in the nuclear potential for $30\lesssim Z\lesssim40$. This leads to shell gaps in the nuclear mean field at nucleon numbers 34, 36 (oblate), 34, 38 (prolate), and 40 (spherical) [1]. The reduction in the excitation energy of the first excited state between the $N=Z=36$ system $^{72}_{36}$Kr and the $N=Z=38$ system $^{76}_{38}$Sr has been interpreted [1–4] as being due to a sudden alteration in the nuclear shape, from deformed oblate in ^{72}Kr to deformed prolate in ^{76}Sr. Lister *et al.* [2] have used the Grodzins estimate to establish that the most deformed nucleus in the region is $^{76}_{38}$Sr$_{38}$ with a prolate deformation of $\beta_2>0.4$. The coexistence of neighboring oblate and prolate shell gaps also causes the nuclear deformation to change dramatically with the addition or subtraction of only a few nucleons. This effect is enhanced in nuclei with near equal numbers of protons and neutrons as the single particle spectra are similar for the two types of nucleon. The nuclear shape can also vary with excitation energy and spin as well as nucleon number. Competition between prolate, oblate, and spherical shapes has been investigated in this region and convincing evidence for shape coexistence between prolate and spherical shapes has been found in ^{76,78}Kr [5,6]. The influence of the positive parity $g_{9/2}$ single particle intruder orbital on the structure of these mass 80 nuclei also becomes apparent when investigating states with oblate deformation in nuclei in this region. Isomeric states arising from the $g_{9/2}$ single particle orbital have been observed in ^{69,71}Se [7] and have been associated with oblate deformed configurations.

The observation of isomeric states allows the investigation of nuclear phenomena such as shape coexistence since they provide information regarding the excitation energies of intrinsic states. This provides a crucial test of mean field models far from the valley of β stability where theoretical descriptions are often extrapolations of data pertaining to near-stable nuclei. The investigation of isomeric states provides information about the competition between single particle and collective structures in nuclei at, or close to, the proton drip line. Information regarding isomeric states present in the neutron deficient mass 80 nuclei is also essential for our understanding of the path of the rp process [8].

The projectile fragmentation of heavy ion beams has been shown to be an excellent mechanism for the production of exotic nuclei due to the high degree of selectivity provided by modern projectile fragment separators such as the LISE3 spectrometer at GANIL [9], the A1200 at MSU [10] and the FRS at GSI [11]. Because of the short flight time from production to detection (typically less than 1 μs), the technique is particularly suited to the study of isomeric states in exotic nuclei.

*Present address: Department of Physics, Florida State University, Tallahassee, FL 32306.
†Present address: Department of Physics, University of Notre Dame, IN 46556.

In the current work, we report the observation of isomeric decays following the fragmentation of a ^{92}Mo beam. Preliminary results of this work have been reported in Refs. [12,13].

II. EXPERIMENTAL TECHNIQUE

The nuclei of interest were produced via the fragmentation of a ^{92}Mo beam of energy 60 MeV/nucleon provided by the GANIL facility. The primary beam, chosen since it is the most neutron deficient stable isotope of this element, had a typical on-target intensity of 100 enA in charge state $Q=37^+$ and was incident on a selection of natural nickel targets of thicknesses between 50 and 100 mg/cm^2. The secondary beam, consisting of the fragmentation products, was separated from the primary beam particles using the LISE3 spectrometer [9] and identified using a combination of time-of-flight, total energy, and energy loss measurements. At the final focus of the spectrometer the fragments were stopped in a four element silicon detector telescope, the first element of which was 300 μm thick and acted as an energy loss (ΔE) detector. The remaining three Si detector elements, each of thickness 150 μm, were used to stop the fragments and also to obtain a total kinetic energy measurement to resolve any charge state anomalies. The magnetic rigidity ($B\rho$) of the main dipole magnets of the LISE3 spectrometer gave a momentum selection for the fragments which, together with the measured time of flight (TOF), energy loss (ΔE), and total kinetic energy (TKE) was used to obtain an unambiguous identification in mass A, proton number Z, and charge state Q for each fragment using the technique described in Refs. [14–17]. The typical time of flight for the fragments between the production target through the spectrometer to the silicon telescope was measured to be approximately 480 ns. An achromatic beryllium degrader of thickness 50 μm and a Wien filter were used to select the most exotic isotopes for study at the final focus of the spectrometer. An array of seven high purity germanium detectors of 70% relative efficiency was packed in close geometry around the silicon stack to measure γ decays from isomeric states in the fragments. The absolute photopeak efficiency of this array was measured using ^{133}Ba and ^{152}Eu sources to be approximately 3% for a 1.33 MeV γ ray. Increased detection efficiency for low-energy γ-ray decays was obtained by using a four element germanium detector (LEPS). A layer of lead was inserted around each detector to absorb scattered γ rays. This gave rise to some contamination of the short time gated isomers due to time walk of the prompt Pb x rays.

III. DATA ANALYSIS AND PARTICLE IDENTIFICATION

The initial isotopic identification was achieved by creating a two dimensional spectrum of correlated energy loss (ΔE) and time-of-flight (TOF) signals for each fragment. In order to obtain an identification plot of Z vs A/Q, it was first necessary to calibrate the energy losses in the silicon detectors. This was accomplished by studying a number of isotopes from the two regions of interest. Following preliminary particle identification (ΔE-TOF) the energy signals in each

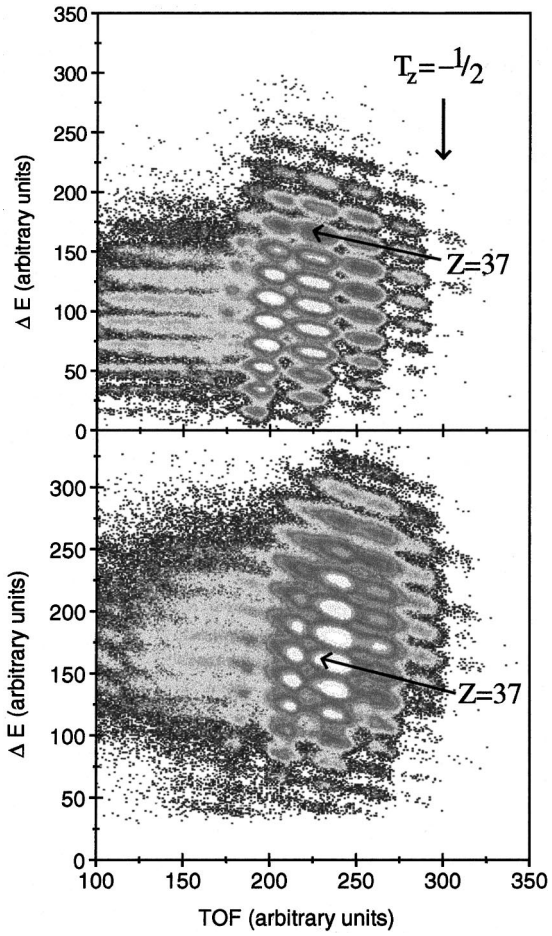

FIG. 1. Particle identification plots of energy loss in the first silicon (ΔE) verses time of flight (TOF) for two separate spectrometer settings. Both an achromatic degrader and a Wien filter were employed to enhance the region of interest. The settings for the top spectrum were $B\rho_1=1.9501$ Tm and $B\rho_2=1.9068$ Tm, the bottom spectrum had the same value of $B\rho_2$ but $B\rho_1$ was changed to 1.9574 Tm.

of the four silicon detectors were compared to the energy loss values calculated by the LISE3 fragmentation and transmission code for each nucleus [18]. The energy losses are calculated according to the prescription provided by Hubert *et al.* [19]. A comparison of the calculated energy loss and silicon detector signal for a number of isotopes allowed the silicon detectors to be calibrated via a polynomial fit.

In order to focus on specific nuclei of interest it was necessary to optimize the spectrometer settings. In the present study a number of different settings was used to search for isomers in an extended region of nuclei and the ΔE-TOF plots for two of the main settings before $(Z,A/Q)$ calibration are shown in Fig. 1. Once calibrated for Z and A/Q it was possible to combine all of the data into one plot as shown in Fig. 2.

Information on the decay half-lives of isomeric states was achieved by recording the time interval between an ion implantation and the detection of a γ ray. Two time ranges, of $0\rightarrow600$ ns (TDC) and $0\rightarrow80$ μs (TAC), were used to allow good temporal resolution over a wide time range. The master

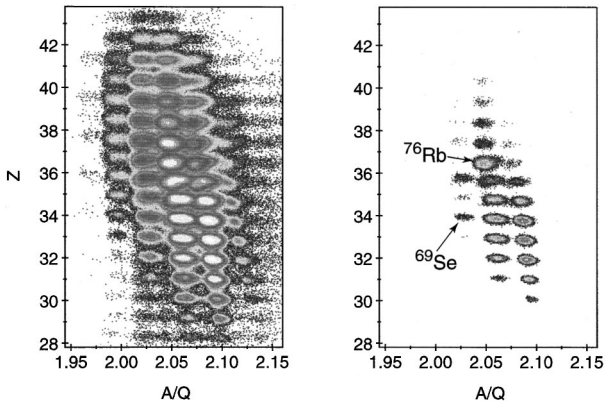

FIG. 2. Calibrated particle identification plots of Z vs A/Q incorporating (a) all of the data from all spectrometer settings and (b) nuclei in coincidence with a delayed γ ray in the range $(0.2 \leqslant \Delta t \leqslant 10)$ μs.

trigger required a signal from the ΔE detector which started the TACs and TDCs. A two-dimensional plot of time measured in the TDCs versus γ-ray energy in the large germanium detectors is shown in Fig. 3. Figure 3(a) shows the effect of correcting for low energy time walk in the detectors in the offline analysis using a polynomial to linear transformation [see Fig. 3(b)]. These spectra were used to exclude the prompt transitions in offline analysis, thereby allowing clean, delayed γ-ray spectra to be obtained for each isotopic species. Decays from previously reported isomers in ^{67}Ge [20], ^{69}Se [21], and ^{76}Rb [22] were identified and the results obtained are consistent with previously reported lifetime values for these nuclei (see Fig. 4). These nuclei were used to provide an unambiguous calibration of the particle identification spectrum (see Fig. 1) and also for internal consistency checks for γ-ray energies and timing.

IV. RESULTS

An initial search for isomeric states can be facilitated by means of an identification plot such as Fig. 2, where any heavy ion event in coincidence with a delayed γ-ray (detected at least 20 ns after the prompt component) increments the spectrum. In this way, isomers can be highlighted, as shown on the right hand side of Fig. 2. This technique has been used previously to search for isomers in a large number of nuclei simultaneously [14].

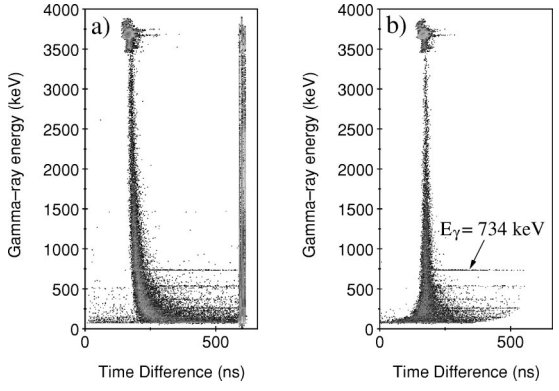

FIG. 3. Two dimensional plots of (a) raw γ-ray energy vs time in the TDCs, and (b) the corrected spectrum, compensated for time walk of low energy γ rays. Note the presence of the delayed transition at 734 keV corresponding to the known isomeric decay in ^{67}Ge (see Fig. 4).

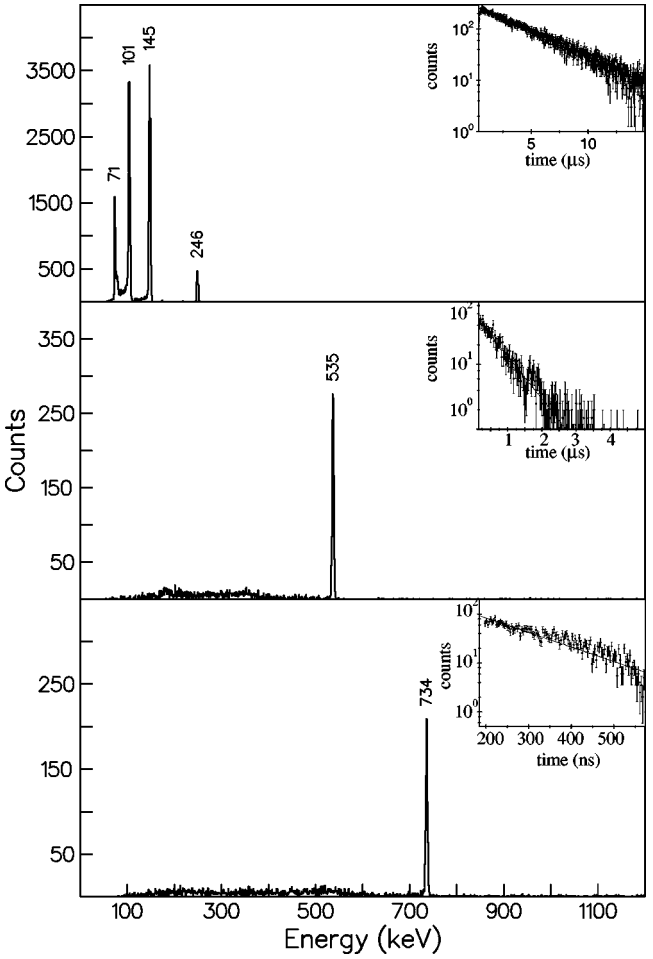

FIG. 4. γ rays deexciting isomeric states in ^{67}Ge (bottom) [20], ^{69}Se (middle) [21], and ^{76}Rb (top) [22] and their associated decay curves, gated on the 734, 535, and 101, 145, and 246 transitions, respectively. The lifetimes obtained in this work are (146 ± 4) ns $[(20 \leqslant \Delta t \leqslant 260)$ ns], (1.37 ± 0.03) μs $[(0.05 \leqslant \Delta t \leqslant 5)$ μs] and (4.40 ± 0.01) μs $[(0.5 \leqslant \Delta t \leqslant 7.6)$ μs], respectively. The numbers in parentheses represent the times ranges following the prompt peak over which the γ-ray spectra were taken.

The projections of the particle identification plots onto the Z axis for the $T_Z = 0$, $\frac{1}{2}$, 1, and $\frac{3}{2}$ species are shown in Fig. 5. The top two sections of each panel require a coincidence with at least one delayed γ ray, so that any nuclei with microsecond isomeric states are enhanced in these plots. In order to discriminate between short lived (20$\rightarrow$400 ns, top section of Fig. 5) and longer lived isomers (0.4$\rightarrow$10 μs, middle section of Fig. 5) two different time ranges were used. In addition to previously identified isomers in less exotic systems, this comparison shows evidence for isomeric states in the $T_Z = 1$ nuclei $^{80}_{39}$Y and $^{84}_{41}$Nb, and the $T_Z = \frac{1}{2}$ nucleus ^{73}Kr. Figure 5 also suggests tentative evidence for isomeric states

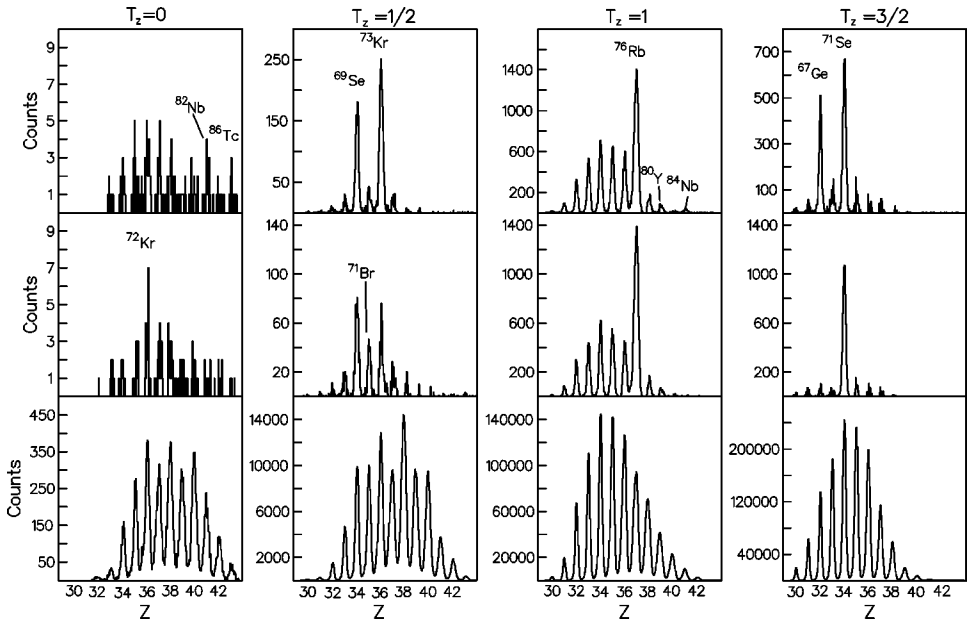

FIG. 5. Projections of $T_Z=0$, $\frac{1}{2}$, 1, $\frac{3}{2}$ nuclear species onto the Z axis for the identification plot shown in Fig. 2. The bottom row of spectra shows all recorded nuclei, the middle row is for long lived isomers in the time region 0.04→10 μs. The top row indicates short lived (20→400 ns) isomeric states.

in the $T_Z=0$ nuclei $^{82}_{41}$Nb and $^{86}_{43}$Tc, the latter of which is discussed in Sec. V C. An example of the sensitivity of using this technique to search for isomers can be observed by noting the change in intensity of the peaks corresponding to ^{67}Ge and ^{71}Se in the top and middle spectra for the $T_z=\frac{3}{2}$ nuclei in Fig. 5, which represent different time regions. This highlights the fact that the lifetime of the decay from the isomeric state observed in ^{67}Ge is much shorter than that of ^{71}Se [146(4) ns: 27(0.7) μs]. All half lives have been fitted using the maximum likelihood method [23] unless otherwise stated.

Isomeric ratio measurements. The isomeric ratio F is defined in the present work as the ratio of the number of ions created in an isomeric state (N_{isomer}) to the total number of ions of a particular nuclide created (N_{ions}), i.e.,

$$F=\frac{N_{\text{isomer}}}{N_{\text{ions}}}=\sum_i F_i, \tag{1}$$

where i represents the number of delayed γ rays observed and the number of ions created in the isomeric state must be corrected for internal conversion (α) and in-flight losses

$$N_{\text{isomer}}=\sum_i \frac{N_{\gamma_i}}{\epsilon_i}\frac{(1+\alpha_i)}{e^{-(t/\tau_{\text{eff}})}}, \tag{2}$$

where N_γ is the intensity of the gamma decay from the isomeric state measured in the germanium detectors, ϵ is the absolute efficiency of the detector at the energy of the isomeric transition. The in-flight loss correction is given by $e^{-t/\tau_{\text{eff}}}$ where t is the time of flight, τ_{eff} is the effective lifetime of the isomeric state for fully stripped ions and is given by

$$\tau_{\text{eff}}=\tau\left(1+\sum_i b_{\gamma_i}\alpha_i\right), \tag{3}$$

where b_{γ_i} is the branching ratio of the ith decay of the state and α_i are the individual internal conversion coefficients for each atomic shell.

It has been observed [14] that the population of yrast and nonyrast isomeric states in intermediate energy projectile fragmentation reactions varies significantly, with yrast states being favored. Values of the isomeric ratio for nuclei produced using fragmentation reactions have been found to range dramatically from case to case [14,28]. Indeed, the production of nuclei in their isomeric state has been found to be dependent on the reaction mechanism and the velocity of the fragment compared to that of the beam [29]. Table I shows the experimentally derived isomeric ratios for the isomers observed in the current work.

V. DISCUSSION

In the following discussion a number of total Routhian surface (TRS) calculations have been performed at rotational frequency = 0.0 MeV/$\hbar$ in order to predict the deformation present in each case and provide a model for the single particle structure in the vicinity of the Fermi surface. In these calculations the total energy is composed of a macroscopic part, which is obtained from the liquid drop model [24], and a microscopic part resulting from the Strutinsky shell correction [25,26]. This method has previously been used to describe K isomers in the $A\sim180$ region [27]. Single particle levels have been calculated using a nonaxial deformed Woods-Saxon potential [1], using the β_2, β_4, and γ deformations predicted for the various minima produced in the calculations.

TABLE I. Summary of isomeric lifetimes and calculated isomeric ratios (F) obtained from this work.

Nucleus	Mean lifetime	E_γ (keV) [a]	$I_i^\pi \rightarrow I_f^\pi$	F (%)	Transmitted ion rate (hr^{-1})
$^{67}_{32}$Ge	(146±4) ns	734	$\frac{9}{2}^+ \rightarrow \frac{5}{2}^-$	60.4±2.6	116 000±6800
$^{69}_{34}$Se	(1.37±0.03) μs	534	$\frac{9}{2}^+ \rightarrow \frac{5}{2}^-$	54.5±2.0	9950±580
$^{71}_{34}$Se	(27.4±0.7) μs	260	$\frac{9}{2}^+ \rightarrow \frac{5}{2}^-$	36.8±1.5	117 600±580
$^{76}_{37}$Rb	(4.40±0.01) μs	71	$4^+ \rightarrow 3^-$	26.7±0.4	71 600±4200
$^{73}_{36}$Kr	(155±15) ns	66	$\frac{9}{2}^+ \rightarrow \frac{7}{2}^-$	75±20	9300±550
$^{74}_{36}$Kr	(42±8) ns	456	$2^+ \rightarrow 0^+$	0.16±0.03 [b]	46 200±2700
$^{80}_{39}$Y	(6.8±0.5) μs	84	$(2^+) \rightarrow 1^-$	10.4±0.8	3800±220
$^{86}_{43}$Tc	(1.6±0.3) μs	595	$(2^+ \rightarrow 0^+)$	36.3±19.5	4.3±0.3

[a]Direct decay from isomeric state, except for ^{74}Kr and ^{86}Tc.
[b]Not corrected for in-flight losses.

A. $^{80}_{39}Y_{41}$

The γ-ray and time spectra corresponding to an isomeric decay in the $T_Z=1$ nucleus $^{80}_{39}$Y are shown in Fig. 6. The isomeric state is shown to decay via a single transition at 84 keV, shown in Fig. 6, with a lifetime of (6.8±0.5) μs. Tentative evidence for this isomer was previously reported by Grzywacz *et al.* [30] following the fragmentation of a ^{112}Sn beam but a value for the decay lifetime could not be deduced in that work. A spin-parity assignment of 4^- for the ground state of ^{80}Y has recently been reported by Döring *et al.* [31]. The same work also identified a much longer lived (τ=6.78 s) isomeric state decaying via a 228.5 keV γ ray to the ground state. The spin and parity of the long lived isomer were assigned as 1^- since the lifetime prohibits all transitions with multipolarity less than 3 and an assignment of 7 would make it yrast and therefore strongly populated in fusion evaporation reactions.

A high spin study [32] using a fusion evaporation reaction found a number of rotational bands in ^{80}Y of which the most intensely populated is assigned at low spin to be a predominantly two quasiparticle $\pi g_{9/2} \otimes \nu g_{9/2}$ configuration. For two of the band heads, the decay cascade connecting directly to the ground state could not be identified, though one of the bands was linked via a single transition to one of the more strongly populated bands. These ''floating'' band heads are candidates for decay via isomeric transitions.

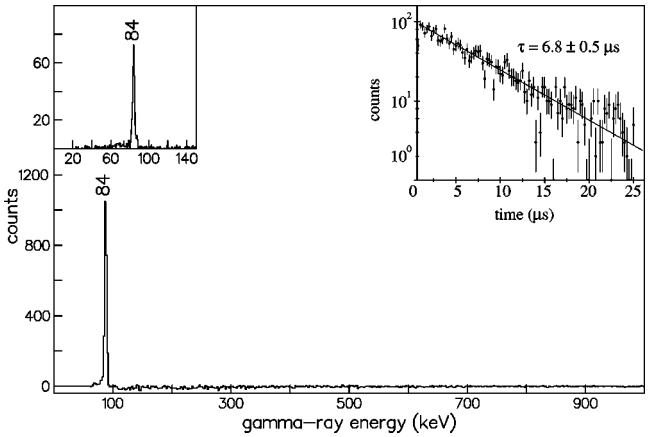

FIG. 6. γ ray and time spectra gated on fully stripped ^{80}Y ions. A single gamma ray is observed at 84 keV. It is also observed in the LEPS spectrum (top left) and has a lifetime of (6.8±0.5)μs (top right). Both γ-ray spectra were taken over a time range of ($0.5 \leqslant \Delta t \leqslant 15$) μs after the prompt peak, and a background subtraction using the long lifetime region of the TAC spectrum has been applied.

The recent work of Döring *et al.* [31] places the 84 keV isomeric transition as decaying out of the 312 keV band head of band 4 suggested by the in-beam study [32]. At the same time they suggest a spin and parity assignment of 2^+ for the band head on the basis of our observations [13]. The earlier assignment of $I^\pi=3^-$ [32] would imply an $E2$ multipolarity for the 84 keV transition to the 1^- state at 228 keV observed in Ref. [31]. The lifetime would correspond to a reduced transition probability for an $E2$ γ ray of 1.38 W.u. However, this assignment would also imply that the 312 keV state could decay by an $M1$ transition to the ground state (the single particle estimates of the half-life of a 312 keV, $M1$ transition of 1 W.u. is 7.24×10^{-13} s) and no such transition is seen in the spectrum shown in Fig. 6. An $M2$ multipolarity for the 84 keV decay is unlikely in view of the corresponding $M2$ strength of $B(M2)=86$ W.u. when compared to the recommended upper limit of 1 W.u. [33]. The combination of transition energy and decay lifetime of the observed 84 keV transition precludes decays with multipolarity of more than 2. The calculated $E1$ and $M1$ strengths for an 84 keV transition correspond to 1.34×10^{-7} W.u. and 8.03×10^{-6} W.u., respectively, which may be compared to the recommended upper limits of 10 mW.u. ($E1$) and 0.5 W.u. ($M1$) [33].

Although an $E1$ assignment suggests a very retarded transition it is still a factor of 4 larger than that observed for an $E1$ decay in ^{79}Se [34] and is similar in strength to the isomeric, $4^+ \rightarrow 3^-$ transition in ^{76}Rb [22]. The retarded $E1$ transition in ^{76}Rb has been interpreted as stemming from different core particle structures. Accordingly the most likely assignment for the 312 keV isomer appears to be $I^\pi=2^+$. We also note that the relatively small value for the measured isomeric ratio for ^{80}Y of 10.4±0.8% (see Table I) is consistent with the nonyrast nature of the isomeric state suggested by Döring *et al.* [31] (see Fig. 7).

The prolate deformed shell gap at nucleon number 38 has a stabilizing effect on the nuclei around ^{80}Y which maxi-

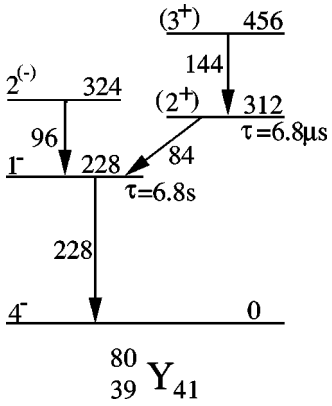

FIG. 7. The low-lying level scheme for ^{80}Y showing the position of the isomeric 312 keV state from the current work and the longer lived, 228 keV state from the work of Döring *et al.* [31]. The energies are given in keV and the tentative spin assignments are given in parentheses.

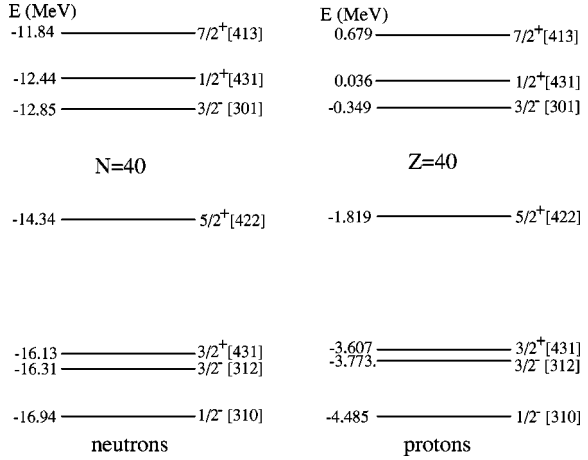

FIG. 9. Calculated single particle levels calculated for ^{80}Y with a positive-parity proton and negative-parity neutron configuration for a deformation of $\beta_2 = 0.385$ and $\gamma = 0°$.

mizes the deformation for the $N = Z = 38$ system ^{76}Sr [2]. In order to estimate the magnitude of the deformation for ^{80}Y, TRS calculations have been performed for both positive-parity proton (neutron) and negative-parity neutron (proton) configurations. Both indicate a large stable prolate deformation, consistent with previous calculations on this nucleus [31]. However, the minimum for the negative-parity neutron, positive-parity proton configuration is significantly lower therefore predicting a ground state deformation of $\beta_2 = 0.385$ (see Fig. 8). Assuming an axially symmetric prolate shape, the single particle energy levels calculated for this configuration (Fig. 9) show that the valence proton and neutron will occupy the $[422]\frac{5}{2}^+$ and $[301]\frac{3}{2}^-$ Nilsson orbitals, respectively. Using the Gallagher-Moszkowski (GM) coupling rules [35], this two-quasi-particle configuration leads to a favored state of spin and parity 4^-. The nonfavored coupling, however, produces a 1^- state which is a candidate configuration for the longer lived isomer [31]. The next available orbital for the odd neutron is $[431]\frac{1}{2}^+$ which favors a residual 2^+ state when coupled to the $[422]\frac{5}{2}^+$ proton orbital. This configuration may correspond to the isomeric state observed in the present work.

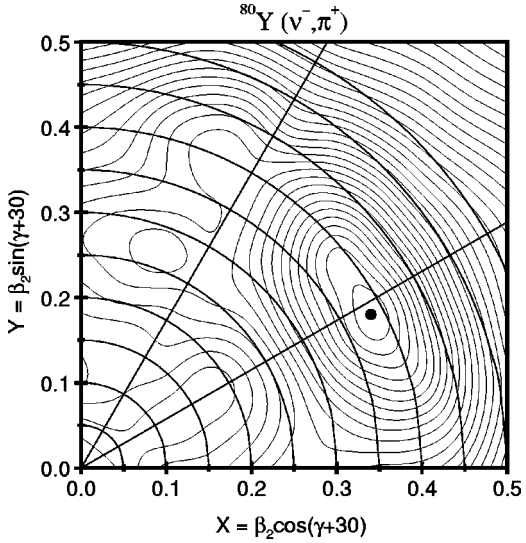

FIG. 8. TRS calculation for the ground state of ^{80}Y for positive-parity proton and negative-parity neutron configuration. The minimum corresponds to deformation parameters of $\beta_2 = 0.385$ and $\gamma = -2.3$. The spacing between contour lines is $\sim$200 keV.

B. $^{84}_{41}Nb_{43}$

The isomeric data observed for the nucleus ^{84}Nb reveal the presence of seven delayed transitions at 47, 65, 115, 133, 141, 175, and 206 keV (Fig. 10). The lifetime has been measured to be (148 ± 28) ns from the 175 keV transition using a least squares fit with a Gaussian shape assumed for the prompt component [36] (Fig. 11).

No coincidence data were available in the current work due to the low counting rate and a high statistics study with in-beam techniques is necessary to corroborate these data.

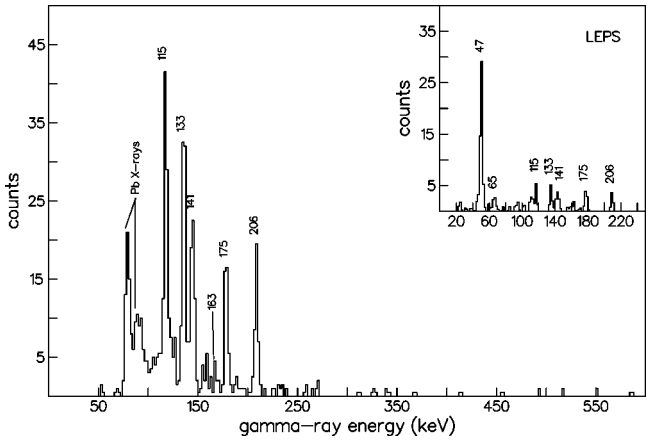

FIG. 10. γ-ray spectra in coincidence with ^{84}Nb ions. The 47 keV transition appears in the LEPS spectrum (top right). Both gamma ray spectra were collected over a time interval of $(50 \leqslant \Delta t \leqslant 800)$ ns after the prompt peak.

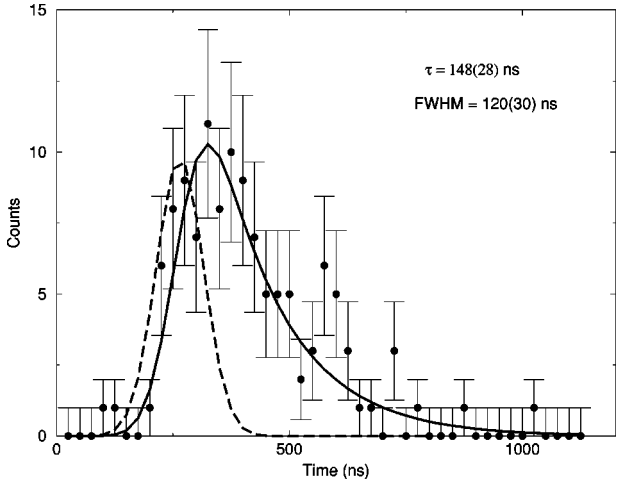

FIG. 11. Lifetime curve obtained from the 175 keV transition observed in ^{84}Nb. The prompt peak (dashed line) has a FWHM of 120±30 ns and the fit gives a lifetime of 148±28 ns.

One such experiment has recently been performed using a thin target [37] and provided both a low-lying level scheme and links to extended high spin bands. An isomeric state at 338 keV ($I^{\pi}=5^{-}$) has been inferred and transitions at 65, 115, 133, 141, 175, and 206 keV have been observed. In that work, a transition at 48 keV is inferred but not observed. As Fig. 10 shows, this transition is present in the current work. The proposed level scheme below the isomeric state at 338 keV is shown in Fig. 12 and shows that the isomeric state decays primarily via the 133 and 175 keV transitions. This thin target experiment [37] was, however, unable to provide a lifetime measurement for the isomer. The intensities in Table II corroborate the ordering of the level scheme (Fig. 12) as well as providing tentative multipolarities for the transitions (given in Table II).

A previous in-beam fusion evaporation study [38] of this $T_Z=1$ nucleus revealed two rotational bands but their positions relative to the ground state were not determined. Band A in Ref. [38] was assigned a $\nu g_{9/2}\otimes\pi(f,p)$ configuration based on similarities with the $\nu g_{9/2}$ band in ^{83}Zr [39]. There were also a number of transitions found that could not be placed in the decay scheme, including two at 114 and 141 keV which were thought possibly to feed isomeric states. This previous work was insensitive to decays from isomeric states but suggests that the transitions at 114 and 141 keV are not direct decays from isomeric states since they were observed in the thin target, in-beam study. As Fig. 12 shows, this is consistent with the interpretation of the current data.

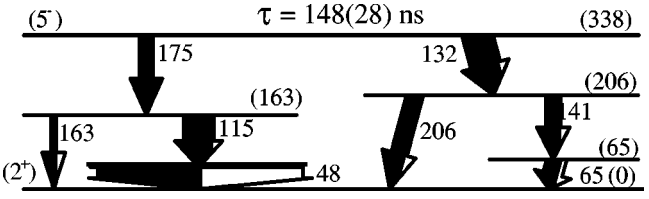

FIG. 12. Low-lying level scheme below the proposed 5^{-} isomer in ^{84}Nb taken from Ref. [37].

TABLE II. Calculated internal conversion coefficients for transitions in $^{84}_{41}$Nb taken from Ref. [43]. I_γ is the γ-ray intensity relative to the 114.7 keV as measured in the large detectors. The tentative multipolarity assignments proposed on the basis of γ-ray intensity balances are given in parentheses. All isomeric ratios have been corrected for in-flight losses assuming a lifetime of 148 ns.

E_γ (keV)	$\alpha(M1)$	$\alpha(E2)$	$\alpha(E1)$	I_γ [a]	F_i (%) [b]
47.4	1.85	16.5	1.00	1570±300 [c]	230±150 ($E1$)
65.0	0.76	5.5	0.42	120±90 [c]	16±13 ($M1$)
114.7	0.15	0.70	0.08	100±15	8.5±2.0 ($E1$)
133.3	0.10	0.41	0.05	76±9	8.4±2.1 ($E2$)
141.4	0.09	0.33	0.04	57±9	4.7±1.2 ($E1$)
175.4	0.05	0.16	0.02	46±7	4.2±1.2 ($E1$)
205.9	0.03	0.08	0.02	49±10	3.9±1.0 ($E1$)

[a]Normalized to the intensity of the 114.7 keV transition.
[b]Corrected for internal conversion assuming multipolarity shown in parenthesis.
[c]Intensity taken from extrapolated LEPS efficiency.

The β^{+}/EC decay of ^{84}Nb was originally studied by Korschinek *et al.* [40] and a lifetime of (12±3) s was extracted for the ground state decay. The decay data revealed a $4^{+}\rightarrow 2^{+}\rightarrow 0^{+}$ yrast cascade in ^{84}Zr and a tentative spin-parity assignment of 3^{+} was made for the ground state of ^{84}Nb by Firestone *et al.* [41]. A more recent study [42] of the decay of ^{84}Nb obtained a ground state decay half-life of (9.5±1.0) s, consistent with the previous value. Döring *et al.* [42] favor a 2^{+} assignment for the ground state based on the population of states in ^{84}Zr, but could not exclude the 1^{+} and 3^{+} possibilities.

In Table II we present the individual isomeric ratios measured for all transitions, with corrections for in flight losses assuming a lifetime of (148±28) ns. The multipolarities have been assigned on the basis of intensity balances and are also given in Table II. We note that the individual isomeric ratios measured for the 115 and 175 keV transitions are consistent with them being in a cascade at the 2σ level. A tentative transition at an energy of 163 keV is indicated in the γ-ray spectrum in Fig. 10 which corresponds to a possible decay from the state fed directly by the 175 keV transition to the ground state.

The possibility that the 47 keV transition decays directly from an independent isomeric state arises when considering its intensity relative to the other transitions (115, 133, 141, and 175 keV), as viewed in the LEPS spectrum (top right of Fig. 10). Its large intensity cannot be balanced with the others, even if electron conversion is taken into account. A measurement of the individual lifetime of the 47 keV transition proved to be unreliable due to low statistics. Therefore the very large isomeric ratio has been deduced to be (230±150)%, assuming a lifetime of (148±28) ns. The large uncertainty stems from the extrapolated value of the efficiency for the LEPS.

The multipolarity of the 65 keV transition has been tentatively assigned as an $M1$, although an $E1$ assignment cannot be ruled out. However, if the 65 keV level is assigned as 3^{-}, one would expect to see an $E2$ transition from the iso-

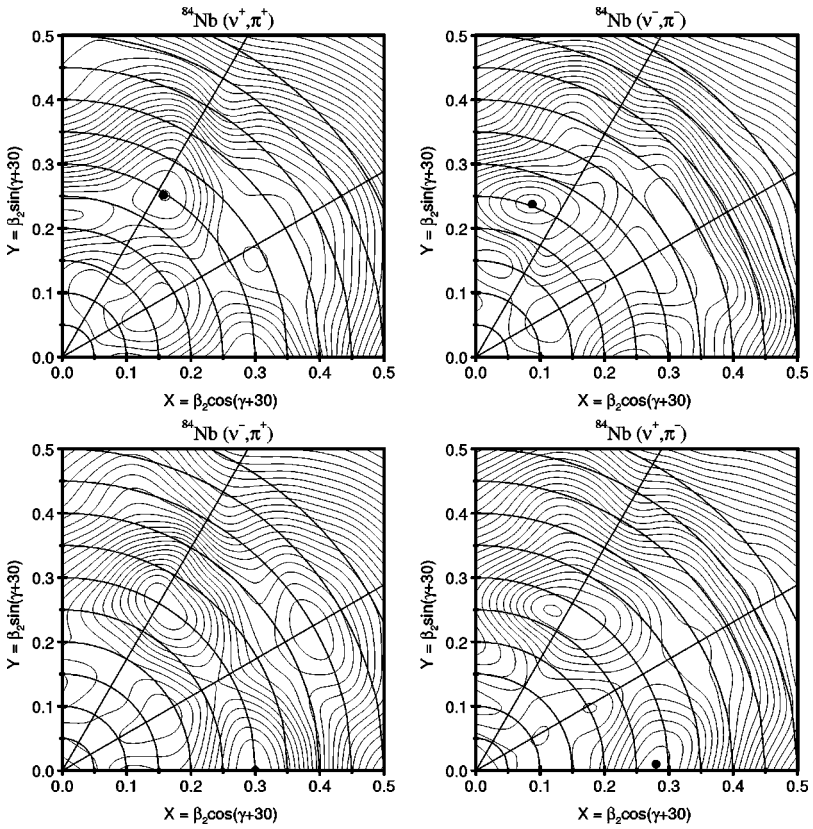

FIG. 13. TRS calculations for ^{84}Nb in the following proton (π) and neutron (ν) parity configurations (clockwise from top left): ($\pi+,\nu+$) ($\beta_2=0.297$, $\beta_4=-0.012$, $\gamma=28.4$), ($\pi-,\nu-$) ($\beta_2=0.254$, $\beta_4=-0.032$, $\gamma=40.5$), ($\pi+,\nu-$) ($\beta_2=0.283$, $\beta_4=-0.015$, $\gamma=-27.5$), ($\pi-,\nu+$) ($\beta_2=0.299$, $\beta_4=-0.013$, $\gamma=-30.0$). The spacing between contour lines is ~200 keV.

meric level at 338 keV, which is not observed. On this basis we prefer an $M1$ assignment, but we note that an unstretched $E1$ is not definitively ruled out.

Total routhian surface calculations for all positive and negative parity configurations have been performed for ^{84}Nb and are shown in Fig. 13. The minima calculated in each case appear to be very close in energy, making it unclear as to which configuration corresponds to the ground state. The quadrupole deformation in each case is significant ($\beta_2=0.285$ and 0.244) with substantial γ deformation ($\gamma\sim30°$). However, we note that other recent shape calculations predict a very small quadrupole deformation of $\epsilon_2=0.05$ [44] for the ground state of ^{84}Nb.

The single particle orbitals corresponding to the calculated deformations in each instance are shown in Fig. 14. The positive parity ground state deduced from β^+/EC decay

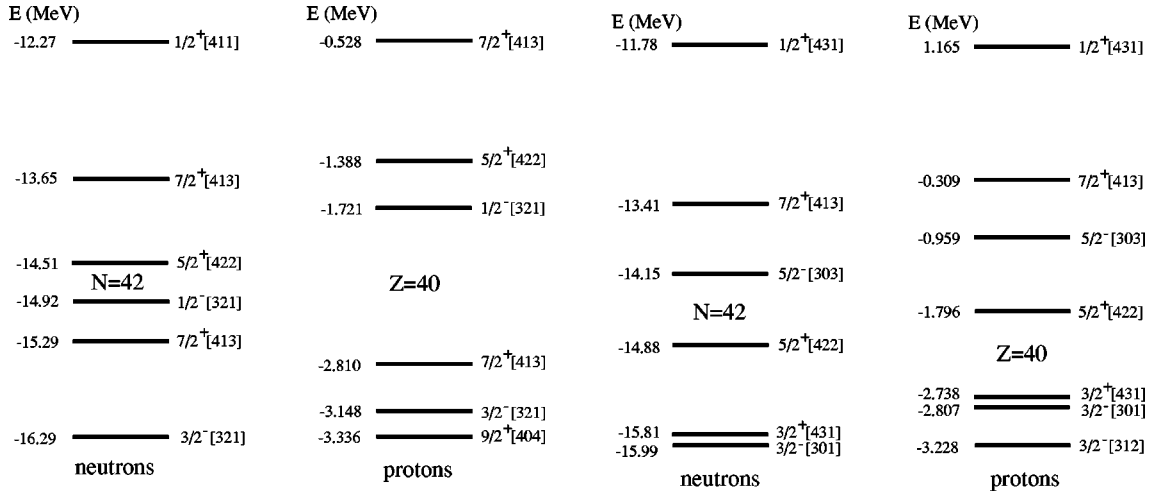

FIG. 14. Single particle levels calculated for the valence proton (π) and neutron (ν) in the following parity configurations—left: ($\pi-,\nu-$) ($\gamma=41°$) and right: ($\pi-,\nu+$), ($\pi+,\nu+$), and ($\pi+,\nu-$) ($\gamma=-30°$).

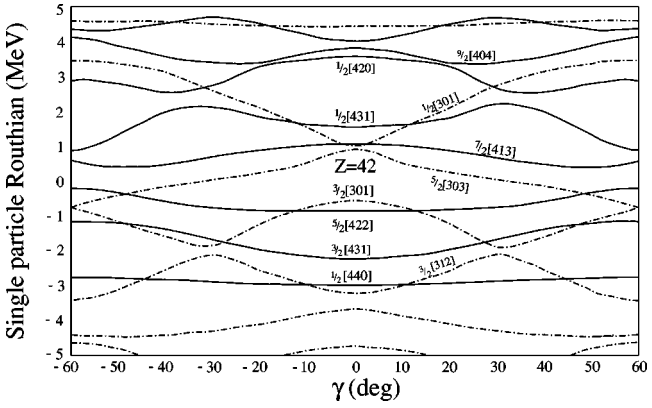

FIG. 15. Proton single particle energy levels as a function of triaxiality for a fixed quadrupole deformation of $\beta_2=0.3$ and $\beta_4=-0.015$. The Nilsson labels have been used as a convenient way of identifying specific orbitals.

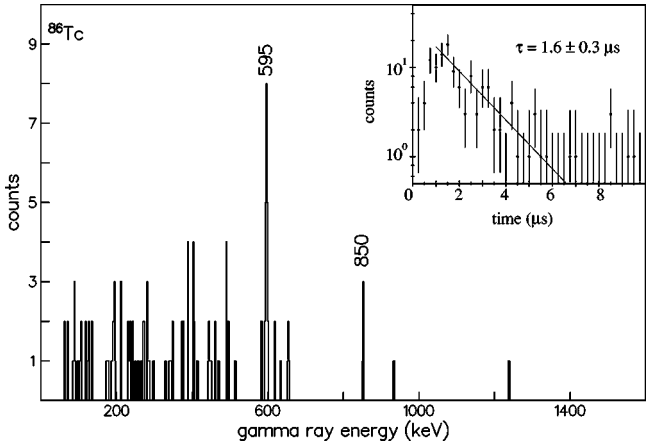

FIG. 16. Tentative transitions in the $N=Z$ nucleus ^{86}Tc at 585 and 850 keV. The associated lifetime is (1.6 ± 0.3) μs and the γ-ray spectrum was taken over the following time range $(0.8\leqslant\tau\leqslant4.2)$ μs.

[42] is not reproduced by our calculations. For the predicted deformed axial minimum with deformation parameters of $\beta_2=0.254$, $\beta_4=-0.032$, and $\gamma=41°$ the lowest lying state would correspond to the favored coupling of the $\nu[422]\frac{5}{2}^+ \otimes \pi[321]\frac{1}{2}^-$ configuration. The Gallagher-Moszkowski coupling rules [35] suggest a preferred 2^- with a 3^- unfavored coupling lying close by. Assuming a 2^+ spin-parity for the ground state of this nucleus, both of the configurations are candidates for the intrinsic structure of the isomeric state at 47 keV, with the yrast 3^- assignment favored in view of the large isomeric ratio.

The right-hand side of Fig. 14 shows the predicted single particle spectra for ^{84}Nb with deformation parameters of $\beta_2=0.298$, $\beta_4=-0.125$, and $\gamma=-29$. We note for this deformation the lowest lying coupling is that of the $\pi[422]\frac{5}{2}^+ \otimes \nu[303]\frac{5}{2}^-$. Although the favored coupling of these orbitals would result in a 0^- state, the unfavored 5^- configuration is a candidate for the structure of the isomeric state at 338 keV.

The complexity of the low-lying single particle structure of this odd-odd nucleus is apparent from the number of states in close proximity beneath the 338 keV isomer. Figure 15 shows the theoretical single particle levels as a function of γ triaxiality which are symmetrical about $\gamma=0°$ and are similar for both protons and neutrons. The level density around nucleon number 42 is predicted to be rather high, possibly explaining the ambiguity as to the configuration of the ground state. The orbitals involved close to the Fermi surface are $\frac{5}{2}^-[303]$, $\frac{7}{2}^+[413]$, and $\frac{1}{2}^-[301]$ for the valence neutron and $\frac{5}{2}^+[422]$, $\frac{5}{2}^-[303]$, and $\frac{7}{2}^+[413]$ for the valence proton. This high level density could also explain the presence of three low-lying isomeric states in this nucleus formed by different couplings of the orbitals around the Fermi surface.

C. $^{86}_{43}$Tc$_{43}$

Figure 16 shows the decay of the isomeric state observed in the $T_Z=0$ nucleus $^{86}_{43}$Tc. The extracted lifetime of this decay is (1.6 ± 0.3) μs with discrete γ-rays of energies 595 and 850 keV (Fig. 16) observed. This nucleus was first identified by Mohar *et al.* [45], but no spectroscopic information has been reported prior to the current work. It is the lightest observed technetium isotope and is the last predicted to be proton bound in the mass evaluation of Audi and Wapstra [46]. Indirect experimental evidence that ^{85}Tc is unbound has been reported by Janas *et al.* [47]. The β^+-decay half-life of ^{86}Tc has been measured by Longour *et al.* [48] to be (47 ± 12) ms and this has been used to infer a spin-parity assignment for the ground state of 0^+ (corresponding to an isospin $T=1$ configuration) from the deduced log ft value [48].

Recent spectroscopic studies of the $N=Z$ nuclei ^{62}Ga [49], ^{66}As [50], and ^{74}Rb [51] have shown $I^\pi=0^+$ $(T=1)$ ground state configurations that are crossed at low excitation energies by higher spin, $T=0$ configurations. Similarities have been seen between these excited $T=0$ bands and the ground state bands of the corresponding $N=Z+2$ isobars which prompts a comparison of ^{86}Tc and its isobaric analog ^{86}Mo.

The $A=86$, $T_Z=1$ system, ^{86}Mo has been studied by Gross *et al.* [52] and Rudolph *et al.* [53]. A positive parity yrast cascade has been established in which the first two excited states lie at 567 and 1328 keV. The yrast $2^+\rightarrow0^+$ transition (567 keV) is close in energy to the observed transition in ^{86}Tc at 595 keV. We also note that the 850 keV γ ray observed in the current work is a candidate for the isobaric analog $4^+\rightarrow2^+$ yrast transition which has an energy of 761 keV in ^{86}Mo [52]. The observed intensity of the 595 keV transition is significantly higher than that of the 850 keV transition suggesting that these states are fed from a higher spin isomer with a fragmented decay path.

The isomeric ratio calculated for the 595 keV transition is given in Table I as $36.3\pm19.5\%$ and implies that the isomeric state is yrast or near yrast and should be well populated in fusion evaporation reactions. The production of this isomer in a $Z=43$ nucleus highlights the fact that the reaction mechanism at these intermediate energies is not pure fragmentation and that pick up reactions can also occur.

Figure 17 shows TRS calculations for ^{86}Tc for the positive parity configuration resulting from the positive-

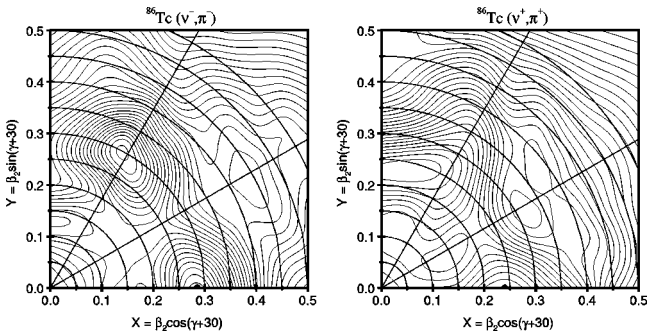

FIG. 17. Configuration constrained potential energy surface calculations for ^{86}Tc. The minima are at 1.28 and 1.22 MeV for the negative-parity (left) ($\beta_2=0.285$, $\beta_4=-0.019$, $\gamma=-29.9$) and positive-parity (right) ($\beta_2=0.244$, $\beta_4=-0.010$, $\gamma=-29.1$) combinations, respectively. The spacing between contour lines is ~200 keV.

(negative-) parity orbitals for both valence nucleons. The minima are close in energy and both infer a triaxially soft, deformed shape for the nucleus with $\beta_2\approx 0.25$. The Nilsson orbitals predicted to lie close to the Fermi surface for both protons and neutrons are $[422]\frac{5}{2}^+$ and $[303]\frac{5}{2}^-$. The population of these orbitals would be expected to give rise to 0^+, 5^+, and 5^- band head configurations. The ground state of this nucleus has been assigned as $I^\pi=0^+$ from measurement of the super allowed β decay half life [48]. This together with the candidate transitions for the $4^+\rightarrow 2^+$ and $2^+\rightarrow 0^+$ decays (850 and 595 keV, respectively) argues in favor of a $I^\pi=5^+$ or 5^- assignment for the isomer. However, this cannot be confirmed in the current work.

D. $^{74}_{36}$Kr$_{38}$

Figure 18 shows the delayed γ-ray transition from the previously reported isomer in ^{74}Kr [12], no delayed transitions were observed in the LEPS spectrum. The isomeric state has been interpreted as being the excited 0^+, predominantly oblate band head predicted for this nucleus [54].

A more recent study [55] of ^{74}Kr, using a combination of conversion-electron and γ-ray spectroscopy, has found evidence for an isomeric $0_2^+\rightarrow 0_1^+$ $E0$ transition corresponding to a state at 508 keV. A lifetime of (20 ± 7) ns was extracted from this later work, consistent, at the 2σ level, with the previous lifetime of (42 ± 8) ns calculated using the maximum likelihood method used for fitting the data away from the prompt peak. When the current data are fitted using a least squares fit with a Gaussian shape assumed for the prompt component [36], a lifetime of (33 ± 7) ns is obtained. The fit is shown on the right hand side in Fig. 18 along with a fit of the prompt component.

The low isomeric ratio measured for ^{74}Kr reflects the nonyrast nature of the isomeric state. The ratio could not be corrected for in-flight losses since the lifetime in flight is hindered due to the ion being fully stripped [12].

E. $^{73}_{36}$Kr$_{37}$

A previous in-beam study [56] of this $T_Z=\frac{1}{2}$ nucleus revealed the presence of an isomeric state at 433.6 keV with limits on the lifetime of between 140 ns and 600 ns. The isomeric state decays initially via a 65.8 keV transition (observed in the present work in the LEPS spectrum, see Fig. 19) and other previously identified transitions at 144, 224, and 368 keV can also be seen in Fig. 19. A lifetime of (155 ± 15) ns has been extracted in the present work for the three most intense transitions at energies of 144, 224, and 368 keV. These transitions are shown in the level scheme in Fig. 20. The previous spin assignments come directly from the observation of the isomeric state, which was assigned as $I^\pi=\frac{9}{2}^+$ since a transition to the ground state was not observed [56]. Other spin assignments were made in Ref. [56] on the basis of DCO ratios. The ground state has been assigned $I^\pi=\frac{5}{2}^-$ from the log ft value of the β decay to levels in ^{73}Br

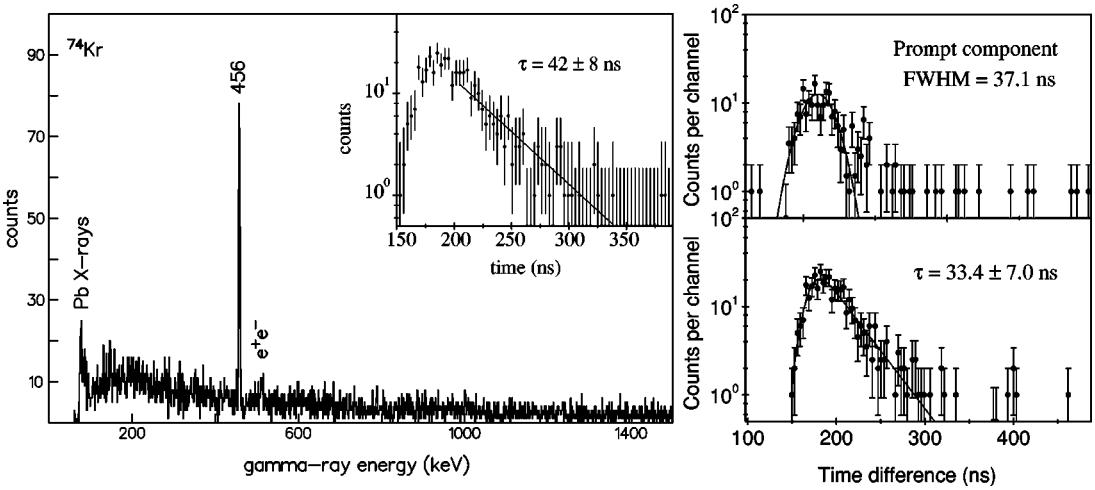

FIG. 18. γ-ray and time spectra for the isomer decay in ^{74}Kr [12]. The lifetime spectrum in the top right of the γ-ray spectrum has been fitted using the maximum likelihood method, whereas the spectrum on the bottom right has been fitted using the least squares method which takes into account the prompt component (shown top right). The gamma ray spectrum was taken between $(0.05\leqslant\tau\leqslant 130)$ ns after the prompt peak.

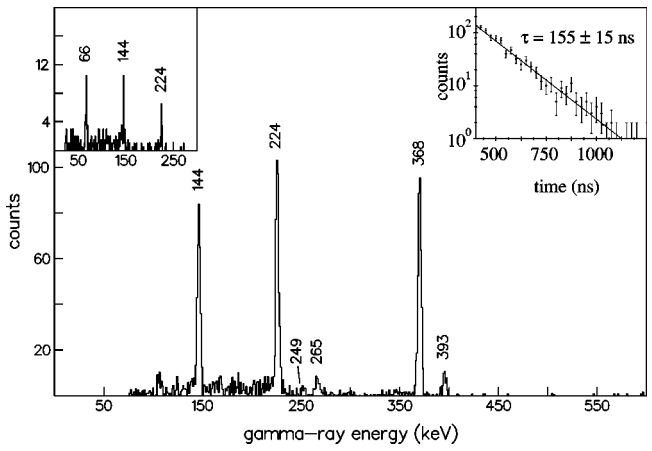

FIG. 19. γ rays following the decay of the isomer in ^{73}Kr. Note the previously unreported transitions at 265 and 393 keV. The spectrum in the upper left corner is from the LEPS. The time spectrum is gated by the intense transitions at 144, 224, and 368 keV. Both γ ray spectra were taken between $(0 \leqslant \tau \leqslant 1)$ μs after the prompt peak.

[57]. However, a recent work has assigned the ground state to be $I^{\pi}=\frac{3}{2}^{-}$ deduced from the β decay to a previously unobserved state in ^{73}Br [58].

The transitions observed, or inferred, in the present work are listed in Table III together with multipolarity assignments from this work and the previous work [56]. Weisskopf single particle estimates suggest that the 65.8 keV transition from the isomeric state is either $E1$ or $E2$, although we note that the $B(E2)$ value would be close to the recommended upper limit. On this basis, an $E1$ multipolarity is favored and the level at 368 keV is assigned $I^{\pi}=\frac{7}{2}^{-}$. Also present in the γ-ray spectrum (Fig. 19) are two transitions at 265 and 393 keV. The latter transition was observed in Ref. [56] but no transition linking it to the isomeric state was reported.

The lifetime measured for the 393 keV transition indicates that the isomeric state feeds this level decaying via a 40.8 keV transition. Assuming the same spin assignments as outlined in Ref. [56] an assignment of $M2$ is suggested for the 40.8 keV transition. The transition would be highly converted (α=41), which is consistent with the nonobservation in the LEPS spectrum (Fig. 19). However, in view of the intensity of the 393 keV transition it is unlikely that the 40.8 keV transition is an $M2$ since it would be hindered and the

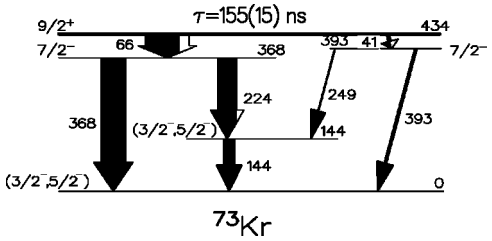

FIG. 20. The low-lying decay scheme depopulating the $\frac{9}{2}^{+}$ isomer in ^{73}Kr, taken partly from Ref. [56]. The 41 keV transition and a revised spin assignment for the 393 keV level are inferred from the present work.

TABLE III. Relative γ-ray intensities (I_{γ}) corrected for detection efficiency, multipolarities, and internal conversion coefficients (α) for γ decays associated with ^{73}Kr. The internal conversion coefficients are taken from Ref. [43] using the multipolarity assignments in the current work.

E_{γ} (keV)	I_{γ}	$I_i^{\pi} \rightarrow I_f^{\pi}$	α [c]
40.8	27±5 [a]	$\frac{9}{2}^{+} \rightarrow \frac{7}{2}^{-}$	1.24
65.8	387±62 [b]	$\frac{9}{2}^{+} \rightarrow \frac{7}{2}^{-}$	0.31
144.2	100±6	$(\frac{3}{2}^{-},\frac{5}{2}^{-}) \rightarrow (\frac{3}{2}^{-},\frac{5}{2}^{-})$	0.048
223.6	166±6	$\frac{7}{2}^{-} \rightarrow (\frac{3}{2}^{-},\frac{5}{2}^{-})$	0.049
248.6	7±2	$\frac{7}{2}^{-} \rightarrow (\frac{3}{2}^{-},\frac{5}{2}^{-})$	0.033
265.1	13±3		
367.8	231±12	$\frac{7}{2}^{-} \rightarrow (\frac{3}{2}^{-},\frac{5}{2}^{-})$	0.009
392.8	22±4	$\frac{7}{2}^{-} \rightarrow \frac{3}{2}^{-}$	0.007

[a]Deduced from $\Sigma I(249+393)$ and $E1$ decay.
[b]Deduced from $\Sigma I(224+368)$ and $E1$ decay.
[c]Assuming the assignment in the current work.

65.8 keV transition would dominate. Reduced transition probability arguments suggest that a multipolarity of $E1$ is more likely for the 40.8 keV transition, changing the assignment of the state at 392.8 keV to $I^{\pi}=\frac{7}{2}^{-}$, which in turn alters the multipolarity of the 248.6 and 392.8 keV transitions to $E2$ and $M1$, respectively. The observation of the weak second decay branch of the isomer via the inferred 41 keV decay highlights the sensitivity of isomer studies such as this and their importance in identifying the low-lying single particle configurations in these very proton rich systems.

The transition at 265.1 keV was not observed in the previous work and has a small intensity in the present work. Although the lifetime measured from the 265 keV transition suggests that it is fed by the main isomeric state, it cannot be definitively assigned since no transition linking it to the ground state is present in the spectrum.

VI. CONCLUSION

Low-lying isomeric states have been populated in the neutron deficient mass 80 nuclei following the fragmentation of a ^{92}Mo beam. Isomeric states have been observed for the first time in the $N=Z+2$ nuclei $^{80}_{39}$Y and $^{84}_{41}$Nb and the $N=Z$ nucleus, $^{86}_{43}$Tc. The precision of the lifetime of the previously reported isomeric state in ^{73}Kr has been improved and evidence of a second decay branch observed.

In the cases of $^{80}_{39}$Y, $^{84}_{41}$Nb, and $^{86}_{43}$Tc, TRS calculations have been performed in order to give an insight into the single particle orbitals present at the Fermi surface which may give rise to isomeric states. The results for ^{80}Y reproduce previous calculations [31], suggesting a $\pi[422]\frac{5}{2}^{+} \otimes \nu[301]\frac{3}{2}^{-}$ configuration for the ground state. The calculations performed for ^{84}Nb predict a triaxial shape for the ground state but are unclear with regard to the preferred single particle configuration of the ground state.

The data presented are an excellent example of how intermediate energy projectile fragmentation reactions can be a

useful tool in nuclear spectroscopy, particularly in the study of nuclei at the limits of particle stability. The simultaneous production and measurement of a large number of nuclides allows the systematic investigation of nuclear structure, in this case, of nuclei in the neutron deficient $A \sim 80$ region. Although this method is limited to the study of isomeric states, the information obtained can be used as a very clean experimental tag, thus allowing a more detailed spectroscopy in future in-beam studies.

ACKNOWLEDGMENTS

This work is supported by EPSRC (U.K.), IN2P3 and CEA (France), the Conseil régional de l'Aquitaine, the Franco-British Research Program (Alliance) and The European Community under Contract No. CHGE-CT94-0056 (Human Capital and Mobility, Access to the GANIL large scale facility). C.C., R.D.P., and S.M.V. acknowledge financial support from EPSRC. B.B. acknowledges support from the Concierge Internationale.

[1] W. Nazarewicz, J. Dudek, R. Bengtsson, and I. Ragnarsson, Nucl. Phys. **A435**, 397 (1985).

[2] C. J. Lister, P. J. Ennis, A. A. Chishti, B. J. Varley, W. Gelletly, H. G. Price, and A. N. James, Phys. Rev. C **42**, R1191 (1990).

[3] W. Gelletly, M. A. Bentley, H. G. Price, J. Simpson, C. J. Gross, J. L. Durell, B. J. Varley, O. Skeppstedt, and S. Rastikerdar, Phys. Lett. B **253**, 287 (1991).

[4] G. de Angelis, C. Fahlander, A. Gadea, E. Farnea, W. Gelletly, A. Aprahamian, D. Bazzacco, F. Becker, P. G. Bizzeti, A. Bizzeti-Sona, F. Brandolini, D. de Acuna, M. De Poli, J. Eberth, D. Foltescu, S. M. Lenzi, S. Lunardi, T. Martinez, D. R. Napoli, P. Pavan, C. M. Petrache, C. Rossi Alvarez, D. Rudolph, B. Rubio, W. Satula, S. Skoda, P. Spolaore, H. G. Thomas, C. A. Ur, and R. Wyss, Phys. Lett. B **415**, 217 (1997).

[5] R. B. Piercy, J. H. Hamilton, R. Soundranayagam, A. V. Ramayya, C. F. Maguire, X.-J. Sun, Z. Z. Zhao, R. L. Robinson, H. J. Kim, S. Frauendorf, J. Döring, L. Funke, G. Winter, J. Roth, L. Cleemann, J. Eberth, W. Neumann, J. C. Wells, J. Lin, A. C. Rester, and H. K. Carter, Phys. Rev. Lett. **47**, 1514 (1981); R. B. Piercey, A. V. Ramayya, J. H. Hamilton, X. J. Sun, Z. Z. Zhao, R. L. Robinson, H. J. Kim, and J. C. Wells, Phys. Rev. C **25**, 1941 (1982).

[6] R. L. Robinson, H. J. Kim, R. O. Sayer, W. T. Milner, R. B. Piercey, J. H. Hamilton, A. V. Ramayya, J. C. Wells, and A. J. Caffrey, Phys. Rev. C **21**, 603 (1980).

[7] M. Wiosna, J. Busch, J. Eberth, M. Liebchen, T. Mylaeus, N. Schmal, R. Sefzig, S. Skoda, and W. Teichert, Phys. Lett. B **200**, 255 (1988).

[8] H. Schatz, A. Aprahamian, B. A. Brown, J. Görres, H. Herndl, K.-L. Kratz, P. Möller, B. Pfeiffer, T. Rauscher, J. F. Rembges, F. K. Thielemann, M. Wiescher, and L. van Wormer, Nucl. Phys. **A621**, 417c (1997); H. Schatz, A. Aprahamian, J. Görres, M. Wiescher, T. Rauscher, J. F. Rembges, F. K. Thielemann, B. Pfeiffer, P. Möller, K.-L. Kratz, H. Herndl, B. A. Brown, and H. Rebel, Phys. Rep. **294**, 167 (1998).

[9] A. C. Mueller and R. Anne, Nucl. Instrum. Methods Phys. Res. B **56/57**, 559 (1991).

[10] B. M. Sherrill, D. J. Morrissey, J. A. Nolen, N. A. Orr, and J. A. Winger, Nucl. Instrum. Methods Phys. Res. B **56/57**, 1106 (1991).

[11] H. Geissel, P. Armbruster, K. H. Behr, A. Brünle, K. Burkard, M. Chen, H. Folger, B. Franczak, H. Keller, O. Klepper, B. Langenbeck, F. Nickel, E. Pfeng, M. Pfützner, E. Roeckl, K. Rykaczewski, I. Schall, D. Schardt, C. Scheidenberger, K.-H. Schmidt, A. Schroter, T. Schwab, K. Sümmerer, M. Weber, G. Münzenberg, T. Brohm, H.-G. Clerc, M. Fauerbach, J.-J. Gaimard, A. Grewe, E. Hanelt, B. Knödler, M. Steiner, B. Voss, J. Weckenmann, C. Ziegler, A. Magel, H. Wollnik, J. P. Dufour, Y. Fujita, D. J. Vieira, and B. Sherrill, Nucl. Instrum. Methods Phys. Res. B **70**, 286 (1992).

[12] C. Chandler, P. H. Regan, C. J. Pearson, B. Blank, A. M. Bruce, W. N. Catford, N. Curtis, S. Czajkowski, W. Gelletly, R. Grzywacz, Z. Janas, M. Lewitowicz, C. Marchand, N. A. Orr, R. D. Page, A. Petrovici, A. T. Reed, M. G. Saint-Laurent, S. M. Vincent, R. Wadsworth, D. D. Warner, and J. S. Winfield, Phys. Rev. C **56**, R2924 (1997).

[13] P. H. Regan, C. Chandler, C. J. Pearson, B. Blank, R. Grzywacz, M. Lewitowicz, A. M. Bruce, W. N. Catford, N. Curtis, S. Czajkowski, P. Dessagne, A. Fleury, W. Gelletly, J. Giovinazzo, Z. Janas, C. Longour, C. Marchand, C. Miehe, N. A. Orr, R. D. Page, M. S. Pravikoff, A. T. Reed, M. G. Saint-Laurent, S. M. Vincent, R. Wadsworth, D. D. Warner, and J. S. Winfield, Acta. Phys. Pol. B **28**, 431 (1997).

[14] R. Grzywacz, R. Anne, G. Auger, D. Bazin, C. Borcea, V. Borrel, J. M. Corre, T. Dörfler, A. Fomichov, M. Gaelens, D. Guillemaud-Mueller, R. Hue, M. Huyse, Z. Janas, H. Keller, M. Lewitowicz, S. Lukyanov, A. C. Mueller, Yu. Penionzhkevich, M. Pfützner, F. Pougheon, K. Rykaczewski, M. G. Saint-Laurent, K. Schmidt, W.-D. Schmidt-Ott, O. Sorlin, J. Szerypo, O. Tarasov, J. Wauters, and J. Zylicz, Phys. Lett. B **355**, 439 (1995).

[15] B. Blank, S. Andriamonje, S. Czajkowski, F. Davi, R. Del Moral, J. P. Dufour, A. Fleury, A. Musquére, M. S. Pravikoff, R. Grzywacz, Z. Janas, M. Pfützner, A. Grewe, A. Heinz, A. Junghans, M. Lewitowicz, J. E. Sauvestre, and C. Donzaud, Phys. Rev. Lett. **74**, 4611 (1995).

[16] K. Rykaczewski, R. Anne, G. Auger, D. Bazin, C. Borcea, V. Borrel, J. M. Corre, T. Dörfler, A. Fomichov, R. Grzywacz, D. Guillemaud-Mueller, R. Hue, M. Huyse, Z. Janas, H. Keller, M. Lewitowicz, S. Lukyanov, A. C. Mueller, Yu. Penionzhkevich, M. Pfützner, F. Pougheon, M. G. Saint-Laurent, K. Schmidt, W. D. Schmidt-Ott, O. Sorlin, J. Szerypo, O. Tarasov, J. Wauters, and J. Zylicz, Phys. Rev. C **52**, R2310 (1995).

[17] M. Lewitowicz, R. Anne, G. Auger, D. Bazin, C. Borcea, V. Borrel, J. M. Corre, T. Dorfler, A. Fomichov, R. Grzywacz, D. Guillemaud-Mueller, R. Hue, M. Huyse, Z. Janas, H. Keller, S. Lukyanov, A. C. Mueller, Yu. Penionzhkevich, M. Pfutzner, F. Pougheon, K. Rykaczewski, M. G. Saint-Laurent, K. Schmidt, W. D. Schmidt-Ott, O. Sorlin, J. Szerypo, O. Tarasov, J. Wauters, and J. Zylicz, Phys. Lett. B **332**, 20 (1994).

[18] D. Bazin and O. Sorlin, Programme LISE, 1993 (unpublished).
[19] F. Hubert, R. Bimbot, and H. Gauvin, At. Data Nucl. Data Tables **46**, 1 (1990).
[20] M. J. Murphy and C. N. Davids, Phys. Rev. C **28**, 1069 (1983).
[21] K. R. Pohl, D. F. Winchell, J. W. Arrison, and D. P. Balamuth, Phys. Rev. C **51**, 519 (1995).
[22] S. Hofmann, I. Zychor, F. P. Hessberger, and G. Münzenberg, Z. Phys. A **325**, 37 (1986).
[23] S. L. Meyer, *Data Analysis for Scientists and Engineers* (Wiley, New York, 1975), p. 326.
[24] W. D. Myers and W. J. Swiatecki, Ann. Phys. (N.Y.) **84**, 395 (1969).
[25] W. Nazarewicz, M. A. Riley, and J. D. Garrett, Nucl. Phys. **A512**, 61 (1990).
[26] V. M. Strutinsky, Yad. Fiz. **3**, 614 (1966).
[27] F. R. Xu, P. M. Walker, J. A. Sheikh, and R. Wyss, Phys. Lett. B **435**, 257 (1998).
[28] B. M. Young, D. Bazin, W. Benenson, J. H. Kelley, D. J. Morrissey, N. A. Orr, R. Ronningen, B. M. Sherrill, M. Steiner, M. Thoennessen, J. A. Winger, S. J. Yennello, I. Tanihata, X. X. Bai, N. Inabe, T. Kubo, C.-B. Moon, S. Shimoura, T. Suzuki, R. N. Boyd, and K. Subotic, Phys. Lett. B **311**, 22 (1993).
[29] J. M. Daugas, R. Grzywacz, M. Lewitowicz, L. Achouri, J. C. Angelique, L. Axelsson, D. Baiborodin, R. Bentida, R. Beraud, C. Borcea, C. Bingham, W. N. Catford, A. Emsallem, G. de France, H. Grawe, K. L. Jones, R. C. Lemmon, C. Longour, M. J. Lopez-Jimenez, F. de Oliveira-Santos, M. Pfützner, P. H. Regan, K. Rykaczewski, J. E. Sauvestre, M. Sawicka, G. Sletten, and M. Stanoiu, Proceedings of the XXXVII International Winter Meeting on Nuclear Physics, Bormio, p. 395 (1999).
[30] R. Grzywacz, R. Anne, G. Auger, C. Borcea, J. M. Corre, T. Dörfler, A. Fomichov, S. Grevy, H. Grawe, D. Guillemaud-Mueller, M. Huyse, Z. Janas, H. Keller, M. Lewitowicz, S. Lukyanov, A. C. Mueller, N. Orr, A. Ostrowski, Yu. Penionzhkevich, A. Piechaczek, F. Pougheon, K. Rykaczewski, M. G. Saint-Laurent, W. D. Schmidt-Ott, O. Sorlin, J. Szerypo, O. Tarasov, J. Wauters, and J. Zylicz, Phys. Rev. C **55**, 1126 (1997).
[31] J. Döring, H. Schatz, A. Aprahamian, R. C. de Haan, J. Görres, M. Wiescher, W. B. Walters, J. Rikovska, L. T. Brown, C. N. Davids, C. J. Lister, D. Seweryniak, and B. Foy, Phys. Rev. C **57**, 1159 (1998).
[32] D. Bucurescu, C. A. Ur, D. Bazzacco, C. Rossi-Alvarez, P. Spolaore, C. M. Petrache, M. Ionescu-Bujor, S. Lunardi, N. H. Medina, D. R. Napoli, M. De Poli, G. de Angelis, F. Brandolini, A. Gadea, P. Pavan, and G. F. Segato, Z. Phys. A **352**, 361 (1995).
[33] P. M. Endt, At. Data Nucl. Data Tables **23**, 547 (1979).
[34] A. A. Chishti, W. Gelletly, C. J. Lister, B. J. Varley, and Ö. Skeppstedt, J. Phys. G **16**, 431 (1990).
[35] C. J. Gallagher and S. A. Moszkowski, Phys. Rev. **111**, 1282 (1958).
[36] C. Wheldon (private communication); Philip R. Bevington, *Data Reduction and Error Analysis for the Physical Sciences* (McGraw-Hill, New York, 1969), p. 237.
[37] N. Marginean, D. Bucurescu, C. A. Ur, D. Bazzacco, S. M. Lenzi, S. Lunardi, C. Rossi Alvarez, M. Ionescu-Bujur, A. Iordachescu, G. de Angelis, M. De Poli, E. Farnea, A. Gadea, D. R. Napoli, P. Spolaore, and A. Buscemi, Eur. Phys. J. A **4**, 311 (1999).
[38] C. J. Gross, K. P. Lieb, D. Rudolph, M. A. Bentley, W. Gelletly, H. G. Price, J. Simpson, D. J. Blumenthal, P. J. Ennis, C. J. Lister, Ch. Winter, J. L. Durell, B. J. Varley, O. Skeppstedt, and S. Rastikerdar, Nucl. Phys. **A535**, 203 (1991).
[39] D. Rudolph, C. J. Gross, K. P. Lieb, W. Gelletly, M. A. Bentley, H. G. Price, J. Simpson, B. J. Varley, J. L. Durell, O. Skeppstedt, and S. Rastikerdar, Z. Phys. A **338**, 139 (1991).
[40] G. Korschinek, E. Nolte, H. Hick, K. Miyano, W. Kutschera, and H. Morinaga, Z. Phys. A **281**, 409 (1977).
[41] R. B. Firestone and V. S. Shirley, *Table of Isotopes*, 8th ed. (Wiley, New York, 1996).
[42] J. Döring, A. Aprahamian, J. Daly, R. C. de Haan, J. Görres, S. R. Lesher, E. J. Stech, A. Susalla, M. Wiescher, J. J. Ressler, W. B. Walters, J. Uusitalo, C. N. Davids, and D. Seweryniak (private communication).
[43] F. Rösel, H. M. Fries, K. Alder, and H. C. Pauli, At. Data Nucl. Data Tables **21**, 291 (1978).
[44] P. Möller, J. R. Nix, W. D. Myers, and W. J. Swiatecki, At. Data Nucl. Data Tables **59**, 185 (1995).
[45] S. J. Yennello, J. A. Winger, T. Antaya, W. Benenson, M. F. Mohar, D. J. Morrissey, N. A. Orr, and B. M. Sherrill, Phys. Rev. C **46**, 2620 (1992).
[46] G. Audi and A. H. Wapstra, Nucl. Phys. **A595**, 409 (1995).
[47] Z. Janas, C. Chandler, B. Blank, P. H. Regan, A. M. Bruce, W. N. Catford, N. Curtis, S. Czajkowski, Ph. Dessagne, A. Fleury, W. Gelletly, J. Giovinazzo, R. Grzywacz, M. Lewitowicz, C. Longour, C. Marchand, Ch. Miehé, N. A. Orr, R. D. Page, C. J. Pearson, M. S. Pravikoff, A. T. Reed, M. G. Saint-Laurent, J. A. Sheikh, S. M. Vincent, R. Wadsworth, D. D. Warner, and J. S. Winfield, Phys. Rev. Lett. **82**, 295 (1999).
[48] C. Longour, J. Garcés Narro, B. Blank, M. Lewitowicz, Ch. Miehé, P. H. Regan, D. Applebe, L. Axelsson, A. M. Bruce, W. N. Catford, C. Chandler, R. M. Clark, D. M. Cullen, S. Czajkowski, J. M. Daugas, Ph. Dessagne, A. Fleury, L. Frankland, W. Gelletly, J. Giovinazzo, B. Greenhalgh, R. Grzywacz, M. Harder, K. L. Jones, N. Kelsall, T. Kszczot, R. D. Page, C. J. Pearson, A. T. Reed, O. Sorlin, and R. Wadsworth, Phys. Rev. Lett. **81**, 3337 (1998)
[49] S. M. Vincent, P. H. Regan, D. D. Warner, R. A. Bark, D. Blumenthal, M. P. Carpenter, C. N. Davids, W. Gelletly, R. V. F. Janssens, C. D. O'Leary, C. J. Lister, J. Simpson, D. Seweryniak, T. Saitoh, J. Schwartz, S. Tormanen, O. Juillet, F. Nowacki, and P. Van Isacker, Phys. Lett. B **437**, 264 (1998).
[50] R. Grzywacz, S. Andriamonje, B. Blank, F. Boué, S. Czajkowski, F. Davi, R. Del Moral, C. Donzaud, J. P. Dufour, A. Fleury, H. Grawe, A. Grewe, A. Heinz, Z. Janas, A. R. Junghans, M. Karny, M. Lewitowicz, A. Musquère, M. Pfützner, M.-G. Porquet, M. S. Pravikoff, J. E. Sauvestre, and K. Sümmerer, Phys. Lett. B **429**, 247 (1998).
[51] D. Rudolph, C. J. Gross, J. A. Sheikh, D. D. Warner, I. G. Bearden, R. A. Cunningham, D. Foltescu, W. Gelletly, F. Hannachi, A. Harder, T. D. Johnson, A. Jungclaus, M. K. Kabadiyski, D. Kast, K. P. Lieb, H. A. Roth, T. Shizuma, J. Simpson, O. Skeppstedt, B. J. Varley, and M. Weiszflog, Phys. Rev. Lett. **76**, 376 (1996).
[52] C. J. Gross, W. Gelletly, M. A. Bentley, H. G. Price, J.

Simpson, K. P. Lieb, D. Rudolph, J. L. Durell, B. J. Varley, and S. Rastikerdar, Phys. Rev. C **44**, R2253 (1991).

[53] D. Rudolph, C. J. Gross, Y. A. Akovali, C. Baktash, J. Döring, F. E. Durham, P.-F. Hua, G. D. Johns, M. Korolija, D. R. LaFosse, I. Y. Lee, A. O. Macchiavelli, W. Rathbun, D. G. Sarantites, D. W. Stracener, S. L. Tabor, A. V. Afanasjev, and I. Ragnarsson, Phys. Rev. C **54**, 117 (1996).

[54] A. Petrovici, K. W. Schmid, and A. Faessler, Nucl. Phys. **A605**, 290 (1996).

[55] F. Becker, W. Korten, F. Hannachi, P. Paris, N. Buforn, C. Chandler, M. Houry, H. Hübel, A. Jansen, Y. Le Coz, C. F. Liang, A. Lopez-Martins, R. Lucas, E. Mergel, P. H. Regan, G. Schönwasser, and Ch. Thiesen, Eur. Phys. J. A **4**, 103 (1999).

[56] S. Freund, J. Altmann, F. Becker, T. Burkardt, J. Eberth, L. Funke, H. Grawe, J. Heese, U. Hermkens, H. Kluge, K. H. Maier, T. Mylaeus, H. Prade, S. Skoda, W. Teichert, H. G. Thomas, A. von der Werth, and G. Winter, Phys. Lett. B **302**, 167 (1993).

[57] J. Heese, N. Martin, C. J. Gross, W. Fieber, K. P. Lieb, A. Kuhnert, K. H. Maier, and X. Sun, Phys. Rev. C **41**, 1553 (1990).

[58] Ch. Miehé, Ph. Dessagne, Ch. Pujol, G. Walter, B. Jonson, M. Lindroos, and the ISOLDE Collaboration, Eur. Phys. J. A **5**, 143 (1999).